The Determination of Initial Blank Shape by Using the One-step Finite Element Method and Experimental Verification

D. W. Jung and S. J. Lee

(*Submitted 16 February 1999; in revised form 25 October 1999*)

Many process parameters have an effect on the sheet metal forming process. A well-designed blank shape causes the material to flow smoothly, reduces the punch force, and yields a product with a uniform thickness distribution. Therefore, the determination of an initial blank shape plays the important role of saving time and cost in the sheet metal forming process. For these reasons, some approaches to estimate the initial blank shape have been implemented.

In this paper, the one-step approach using a finite element inverse method will be introduced to predict the initial blank shape. The developed program is applied to several sheet metal forming examples for the demonstration of its validity. Moreover, the usefulness of the developed one-step approach program is investigated as compared with the FAST-3D program, which is a commercial package that is commonly used. Finally, the verification will be performed by comparing the predicted and experimental results.

Keywords	experimental verification, finite element method, initial blank shape, one-step approach, process parameter, sheet metal forming

1. Introduction

With the development of computers, much research related to numerical analysis has emerged. The result of this research could even be applied to the sheet metal forming process with very complicated nonlinear problems. As a result, the strain distribution, residual stress, formability of a product, and so on could be known before the sheet material was deformed.

Of the many numerical methods, the incremental finite element method (FEM) is a very accurate one, which can grasp an intermediate path such as history of deformation. However, this method is not suitable to reduce the lead time of the design process because of its long computation time. For this reason, the one-step FEM using the deformation theory of plasticity was developed and will be introduced in this paper.[1]

The one-step method is assumed to deform directly from the initial blank to the final shape without any intermediate process, so this method has a fault—the accuracy is not enough. But the one-step FEM has the advantages of a fast computation speed, an ease of treatment, and an ability to obtain useful information in the product design process. For example, if the initial blank shape is determined in the design process, we can save time and cost by performing trimming work later. And we can also reduce punch force because the material flows smoothly and then obtain a good product of uniform thickness distribution. Therefore, in the product design stage, much study has recently been undertaken to estimate an initial blank shape as well as other process parameters.

D. W. Jung, Dept. of Mechanical Eng., Cheju National University, Cheju-Do, KOREA and **S. J. Lee,** Dept. of Mechanical Eng., Graduate School Course, Cheju National University, Cheju-Do, KOREA.

In this kind of study, the initial blank was calculated by Hazek and Lange,[2] Chu and Dou,[3] and Kuwabara *et al.*[4] using the slip line field method. Vogel and Lee[5] and Chen and Sowerby *et al.*[6] estimated the blank shape by the method of plane stress stress characteristics, and Kim *et al.*[7] analyzed in reverse the process of a material flow from the final shape using the rigid plastic FEM.

The attempt of blank design to use the deformation theory was achieved by Batoz *et al.*[8] They derived a general formulation, which can be applied to a general shape. Also, they estimated the flange shape of final products through the comparison between a predicted blank and a practically produced blank.

In this paper, basic theories of the finite element inverse method will be described, and the one-step FEM based on these theories will be applied to several sheet metal forming examples, such as square cup, cylindrical cup, front fender, and rear hinge forming, for the demonstration of its validity.

2. Description and Formulations of Theory

2.1 Determination of Initial Guess

There is a wide difference generally between the initial blank shape and the final shape. The one-step inverse method is accompanied with high level nonlinear paths. Therefore, the initial guess about the blank shape is needed to obtain the initial blank shape. The method for the initial guess is determined according to the type of given problem, and the calculation can also be solved by mixing methods. First, the vertical projection (z-projection) method[9] can be used to calculate the initial guess. This method projects all coordinates of a final shape vertically on a plane. If the wall of an object is vertical, nodal points on a shape will be overlapped. Therefore, the vertical projection method can only be used in the case of a nonverticality and gentle slope surface.

The method is called geometric mapping,[10] which unfolds all elements of a final shape on a plane equally; hence, the area of

shape is maintained uniformly and has nothing to do with the verticality of the wall. The basis for mapping is best described with the aid of Fig. 1. Figure 1(a) shows the region of mesh located on the surface of a model.

The mapping process is initialized by identifying two start lines, such as lines *abe* and *adf* in the diagram. These lines would generally be lines of symmetry on the product. Now we must locate node *c* in the flat plane, attempting to keep the area of quadrilateral element *abcd* constant. The location is accomplished, as illustrated in Fig. 1(b) to (e).

Figure 2 shows the initial guess of a square cup using the geometric mapping method. A square cup is calculated to be only a

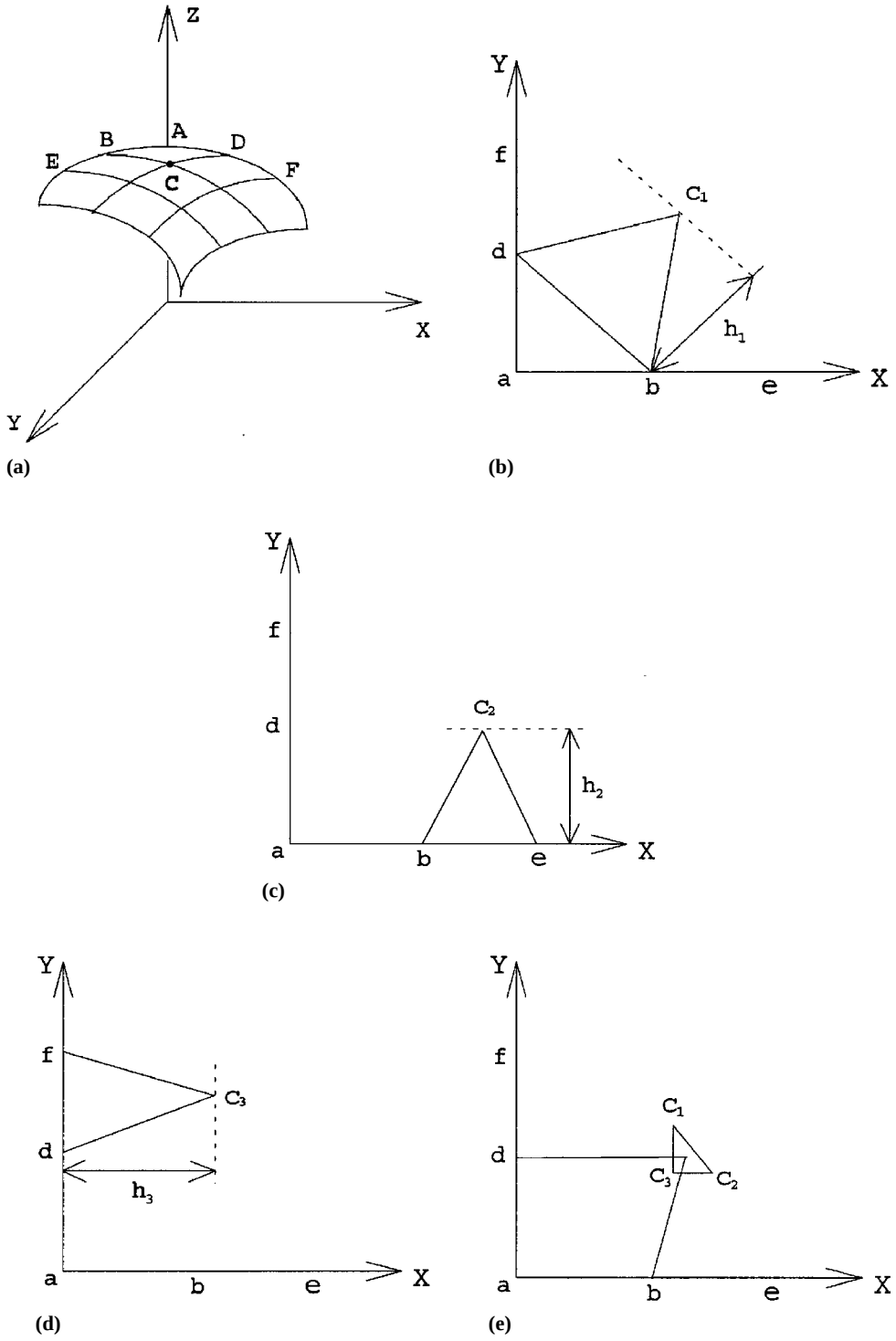

Fig. 1 **(a)** to **(e)** Illustration of the complete mapping procedure

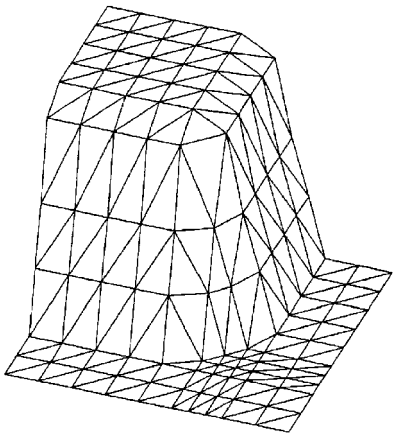

(a)

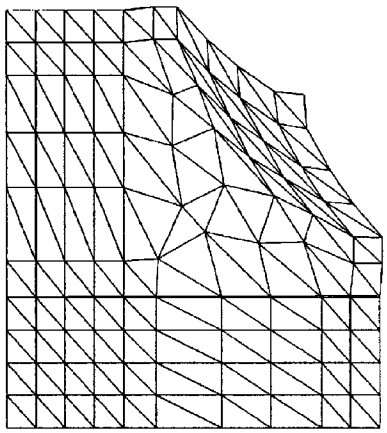

(b)

Fig. 2 The blank shape of a square cup using the geometric mapping method. **(a)** Schematic view of the square cup. **(b)** Calculated initial blank shape

quarter of a total shape, because a square cup is symmetrical about the *X* and *Y* axes.

There are manifold methods to assume the initial guess besides. For example, the design method[11] studied by Lange calculated the initial guess in the field, and the linear inverse projection method,[12] which considers strain rate as a final shape, is elastically unfolded on the plane.

2.2 The One-Step Inverse FEM Formulation

The one-step rigid plastic method using the linear triangular membrane element was proposed for the initial blank design. First, only the initial shape of blank and the desired final shape without consideration of any deformation paths are considered And the initial blank shape of products is calculated on the assumption that the material is deformed from the initial shape to the final shape in the state of minimum potential energy.

This one-step inverse FEM adopts Hill's anisotropic yield criterion[13] and Hencky's deformation theory. And, in the formulation, the triangular membrane element is used, and the

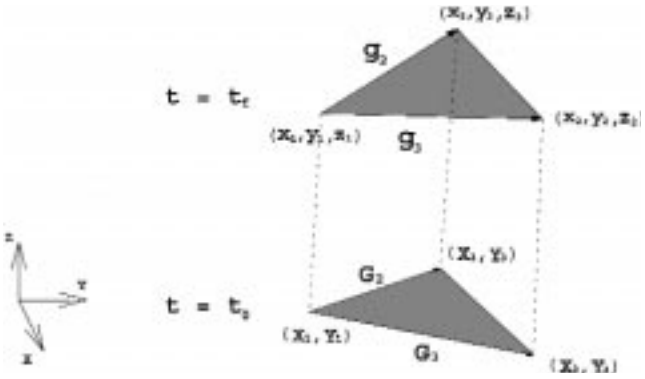

Fig. 3 Kinematics of triangular membrane element between the initial state and the final state

strain expression is expressed only as the function of a coordinate. As in Fig. 3, the triangular element of the initial state can be expressed as vectors of G_{2i}, G_{3i} and the triangular element of final state can be represented as vectors of g_{2i}, g_{3i}. The subscripts such as **2** and **3** refer to the side of a triangular element, and *i* is the *i*th element of the coordinate system.

The deformation gradient *F* can be expressed as the following equation using two vectors (G_{2i}, G_{3i}, and g_{2i}, g_{3i}).

$$F = g_i \cdot G_i^{-1} = \frac{1}{\det}\begin{bmatrix} g_{21} & g_{31} \\ g_{22} & g_{32} \\ g_{23} & g_{33} \end{bmatrix} \cdot \begin{bmatrix} G_{32} & -G_{31} \\ -G_{22} & G_{21} \end{bmatrix} \quad \text{(Eq 1)}$$

In the above equation, det = $G_{21}G_{32} - G_{31}G_{22}$, and two vectors are given by

$$[G_i] = [G_{21}\ G_{22}\ G_{31}\ G_{32}]^T = [X_3 - X_1\ \ Y_3 - Y_1\ \ X_2 - X_1\ \ Y_2 - Y_1]^T$$

$$[gi] = [g_{21}\ g_{22}\ g_{23}\ g_{31}\ g_{32}\ g_{33}]^T = [x_3 - x_1\ \ y_3 - y_1\ \ z_3 - z_1\ \ x_2 - x_1\ \ y_2 - y_1\ \ z_2 - z$$

The Cauchy-Green tensor *C* is represented as Eq. 2 by the deformation gradient *F*. From this equation, the principal elongation λ_1, λ_2 is calculated and then the algebraic strain ϵ_i can be derived such as in Eq. 4.

$$[C] = [F]^T \cdot [F] = \begin{bmatrix} C_{11} & C_{12} \\ C_{21} & C_{22} \end{bmatrix} \quad \text{(Eq 2)}$$

$$\begin{bmatrix} \lambda_1 \\ \lambda_2 \\ \theta \end{bmatrix} = \begin{bmatrix} \sqrt{\frac{(C_1 + C_2)}{2} + \left[\left(\frac{(C_1 - C_2)}{2}\right)^2 + C_3^2\right]^{\frac{1}{2}}} \\ \sqrt{\frac{(C_1 + C_2)}{2} - \left[\left(\frac{(C_1 - C_2)}{2}\right)^2 + C_3^2\right]^{\frac{1}{2}}} \\ \tan^{-1}\left(\frac{\lambda_1 - C_1}{C_3}\right) \end{bmatrix} \quad \text{(Eq 3)}$$

$$[\varepsilon_i(x \text{ or } X)] = \begin{bmatrix} \varepsilon_{xx} \\ \varepsilon_{yy} \\ \varepsilon_{xy} \end{bmatrix} = \begin{bmatrix} 1n\,\lambda_1\,\cos^2\,\theta + 1n\,\lambda_2\,\sin^2\,\theta \\ 1n\,\lambda_1\,\sin^2\,\theta + 1n\,\lambda_2\,\cos^2\,\theta \\ 1n\left(\frac{\lambda_1}{\lambda_2}\right)\sin\theta\cos\theta \end{bmatrix} \quad \text{(Eq 4)}$$

where Hills new yield theory can be represented as follows:

$$\dot{\bar{\varepsilon}} = D_1\left[|\dot{\varepsilon}_1 + \dot{\varepsilon}_2|^{\frac{M}{M-1}} + D_2|\dot{\varepsilon}_1 - \dot{\varepsilon}_2|^{\frac{M}{M-1}}\right]^{\frac{M-1}{M}} \quad \text{(Eq 5)}$$

where $D_1 = 1/2\,[2\,(1 + r)]^{\frac{1}{M}}$ and $D_2 = (1 + 2r)^{\frac{-1}{M-1}}$, where M is an exponent that can describe the yield side in Hill's new yield theory.

The expression of $\dot{\varepsilon}_1 = \ln \dot{\lambda}_1$ and $\dot{\varepsilon}_2 = \ln \dot{\lambda}_2$ is possible because the principal value of the Cauchy-Green tensor can be expressed as the principal strain. Therefore, Eq 5 can be changed as follows:

$$\dot{\bar{\varepsilon}} = D_1\left[\left|\ln\left(\dot{\lambda}_1 \cdot \dot{\lambda}_2\right)\right|^{\frac{M}{M-1}} + D_2\left|\ln\left(\frac{\dot{\lambda}_1}{\dot{\lambda}_2}\right)\right|^{\frac{M}{M-1}}\right]^{\frac{M}{M-1}} \quad \text{(Eq 6)}$$

The representative strain can be expressed as Eq 7 when the material is deformed with the path of minimum work proposed by Chung and Richmond[14] and then Eq 7 is represented as Eq 8.

$$\bar{\varepsilon} = \int_0^{t_f} \dot{\bar{\varepsilon}}\, dt \quad \text{(Eq 7)}$$

$$\bar{\varepsilon} = D_1\left[\left|\ln\left(\lambda_1 \cdot \lambda_2\right)\right|^{\frac{M}{M-1}} + D_2\left|\ln\left(\frac{\lambda_1}{\lambda_2}\right)\right|^{\frac{M}{M-1}}\right]^{\frac{M-1}{M}} \quad \text{(Eq 8)}$$

Also, the representative stress can be defined as follows according to the obtained representative strain:

$$\bar{\sigma} = K(\varepsilon_0 + \bar{\varepsilon})^n \quad \text{(Eq 9)}$$

Therefore, the deformed internal plastic deformation work is calculated as Eq 10 with the defined representative strain and representative stress. Finally, the initial blank shape can be obtained due to the differential values of the plastic work, as in Eq 11.

$$W = \int_{V_0} \bar{\sigma} \cdot \bar{\varepsilon}\, dV_0 \quad \text{(Eq 10)}$$

$$\frac{dW}{dX_i} = 0 \qquad \text{for } i = 1, 2 \quad \text{(Eq 11)}$$

where X_i represents the coordinate of all nodal points in the initial shape.[9] The finite element program based on this formulation was developed, and Fig. 4 shows the flow chart of this developed program. And this program will be applied to several stamping processes for the demonstration of its applicability.

3. The Proof of the One-Step Approach Method through the Experiment

All this while, the estimation of the initial blank shape using the one-step approach method was described. In this section, the validity of this method will be verified by comparing it with the results of the experiment. And the results of the experiment are also compared with the results of the FAST-3D commercial package. The FAST-3D program is used to calculate the initial blank shape by using the one-step approach, which is presented in this study, as well as to predict the state of product after forming—thickness distribution, strain rate, forming severity, *etc*.

The sheet material used in this experiment is an SPC (0.8 mm) panel used generally in the forming experiment, and the material properties are shown in Table 1. The experiment was achieved in the hydraulically operated press unit with the maximum 30 ton blank-holder pressure and the maximum 20 ton punch force. The forming pressure and the deformation depth can be measured by the attached sensor. A photograph of the press used in the experiment is shown in Fig. 5.

3.1 Square Cup Drawing

First of all, the experiment of square cup drawing is performed. Figure 6(a) shows the shape of square cup deformed by the experimental result. Figure 6(b) shows the thickness distribution on the final shape, and Fig. 6(c) is the strain distribution of square cup measured by GPA grid pattern analyzer, CamSys Inc. (Troy, NY) strain measurement equipment. Figure 7 represents a photograph of the GPA equipment. This GPA can measure automatically the strain of material on the surface of a stamped shape.

Table 1 Mechanical property for SPC

Thickness (mm)	*n* value	Yield (kgf/mm²)	Tensile (kgf/mm²)	Elongation (%)
0.8	0.15	20	35	34

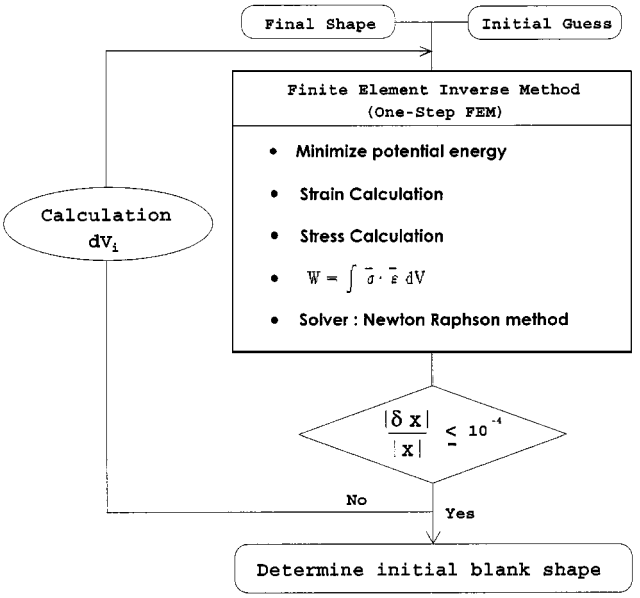

Fig. 4 Flow chart for initial design tool

Fig. 5 Photograph of the press used in this experiment

Figure 8 shows the thickness distribution of square cup analyzed by the FAST-3D code. This is nearly the same result as that achieved with the experiment, that the wall side is thin and the thickness of the flange part is thicker.

3.2 Cylindrical Cup Drawing

Second, the experiment of cylindrical cup drawing is performed. Under the blank holding force of 10 ton, the cylindrical cup is formed until the height of 30 mm is achieved, as shown in Fig. 9.

Figure 10(a) represents, the thickness distribution on the final shape. From this result, we find that the most severe deformation occurs on the wall area and the least deformation occurs in the area contacted with the punch. Figure 10(b) shows the strain distribution of a cylindrical cup by using the forming limit diagram (FLD) curve measured by the GPA equipment. The measurement of strain was taken in the punch face, points 1 to 6, through the side wall, points 7 to 9, onto the die radius, point 10, and in the flange zone, points 11 and 12.

As a result, points 1 to 5 located in the punch face show the plane strain state and the strain is close to zero. Points 7 and 8 show the uniaxial tension state, and point 9 shows the compression state, in the wall side of cylindrical cup, since the material is pulled into the die hole. And we can estimate that the wrinkling will occur in points 9 and 10 from this FLD diagram.

The result by the FAST-3D is shown in Fig. 11 and represents a similar tendency with the result of experiment.

4. Comparison with FAST-3D Commercial Package

In this section, some auto-body panels including the basic shape will be analyzed by using the developed one-step program, and its validity will be examined as compared with the results of FAST-3D code.

4.1 Application to a Square Cup

Figure 12 shows the square cup shape, the height being 60 mm and the width of the flange being 20 mm. The material adopted is

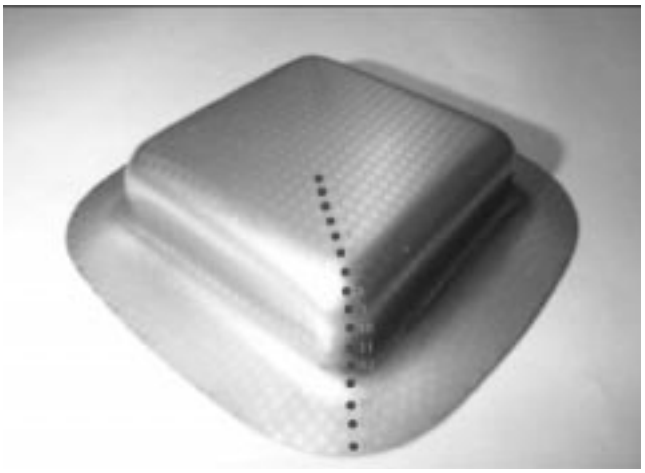

(a)

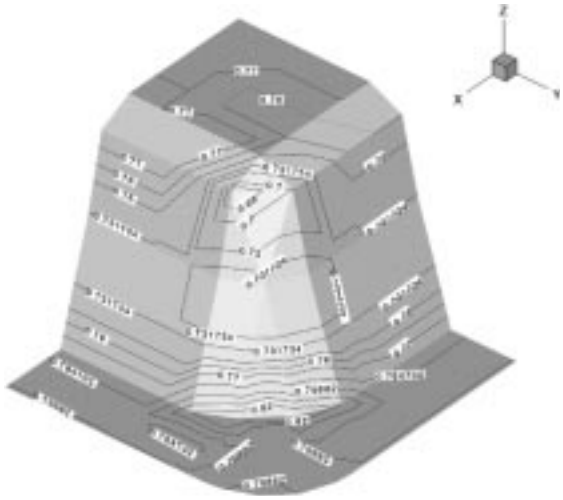

(b)

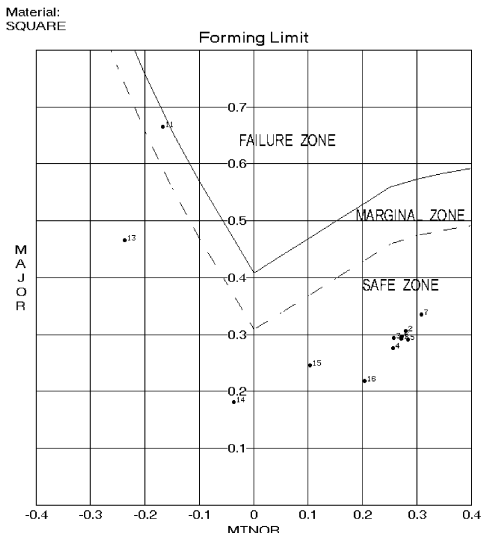

(c)

Fig. 6 The deformed square cup shape by the experiment. **(a)** Photograph of the deformed square cup. **(b)** Measured thickness distributions. **(c)** Measured strain distributions

Fig. 7 Photograph of the strain measurement system (GPA)

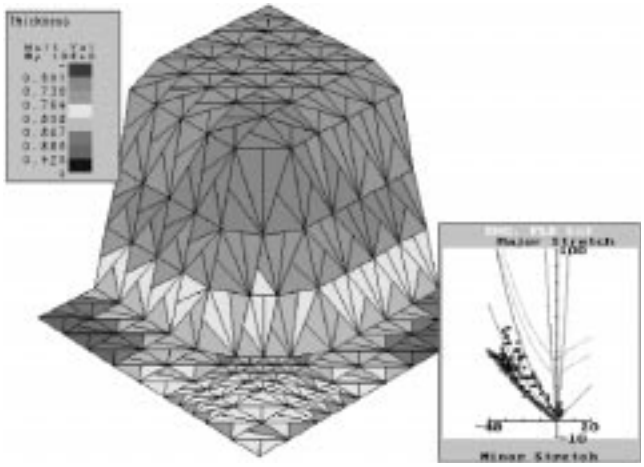

Fig. 8 Predicted thickness distributions by FAST-3D

a cold-heated steel, which is usually used as an auto-body panel. In Table 2, process parameters for the analysis are given.

Figure 13(a) shows an FEM model of a quarter of the square cup shape. The initial guess of square cup shape is determined by the *z* projection introduced in Section 2.1, and the calculated shape is shown in Fig. 13(b). These data will be applied to the developed one-step program.

As the result of the analysis, the calculated geometry is represented as Fig. 14, and the computation time took about 412 s in an IBM RS/6000 43P workstation (IBM, Atlanta, GA).

The computation time of this one-step analysis is very short compared with other FEM analysis methods. The reason is that the calculation is achieved in only one step from the final state to the initial shape.

Figure 15 shows the initial blank shape calculated by FAST-3D. It shows little difference in the corner of the flange compared with Fig. 14 estimated by using the developed program, but the blank shape found by the developed program is analogous to that found by FAST-3D in general.

With combining the analyzed quarter shape, the total initial blank shape before the forming can be estimated as Fig. 16.

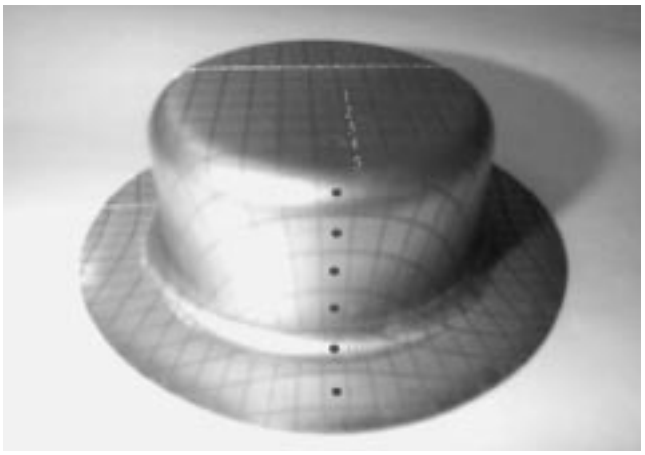

Fig. 9 Photograph of the cylindrical cup drawn

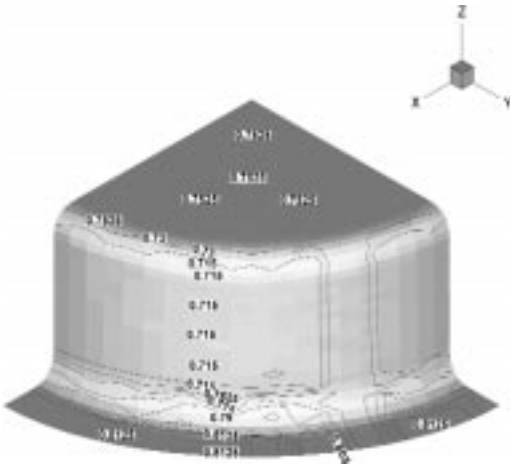

(a)

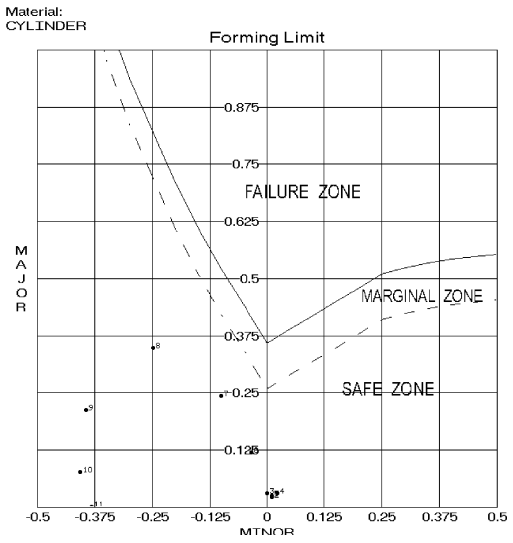

(b)

Fig. 10 The result of the experiment (cylindrical cup drawing). **(a)** Measured thickness distributions. **(b)** Measured strain distributions

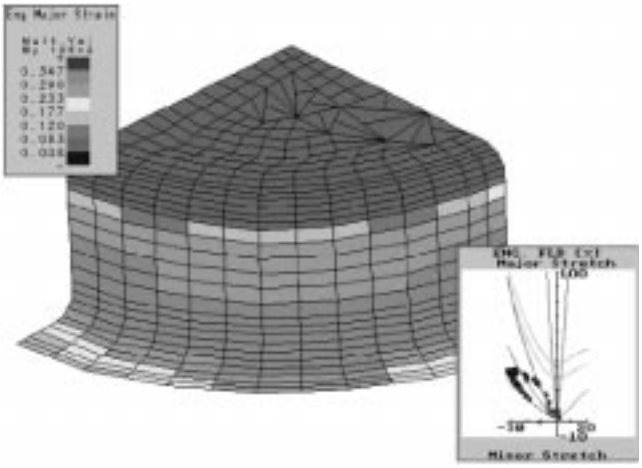

Fig. 11 Predicted strain distributions by FAST-3D

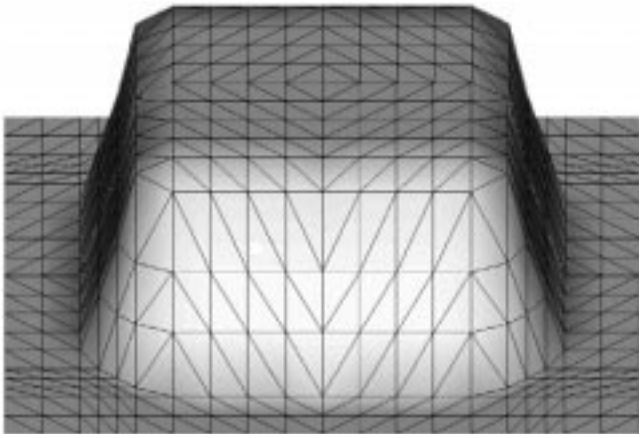

Fig. 12 Schematic view of the square cup

Table 2 Material property (square cup)

Initial material thickness	*n* value	*r* value	Number of nodes	Number of element
0.8 mm	0.185	1.87	121	200

4.2 Application to a Front Fender

In this section, the practical products used in the industrial field are analyzed to demonstrate the applicability and validity of the developed one-step program. The front fender shown in Fig. 17 is one of the parts located in the side of automobile's wheels. The meshed geometry of fender for the analysis is shown in Fig. 18. This shape is composed of a total of 1251 nodes and 2400 triangular elements. The material properties are given in Table 3.

The initial guess of front fender was obtained by the geometric mapping method referred to in Section 2.1. The result of analysis using the one-step method is shown in Fig. 19. The computation time was 520 s in an IBM RS/6000 43P workstation. These results mean that the one-step FEM can also be applied to practical problems with a high level of nonlinear factors such as the front fender.

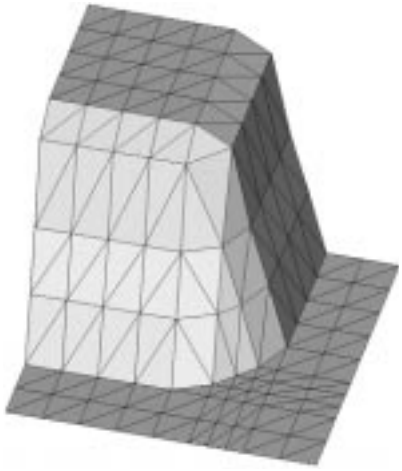

(a)

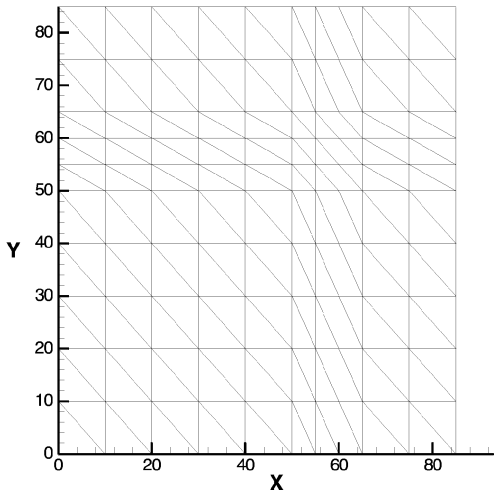

(b)

Fig. 13 FEM model and initial guess of a square cup. **(a)** FEM model of a square cup. **(b)** Calculated initial guess (*z* projection)

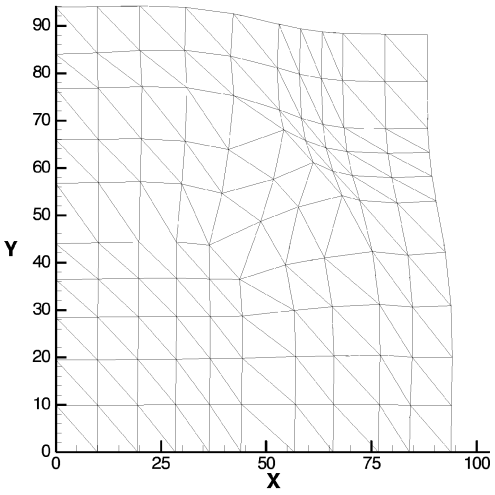

Fig. 14 Calculated initial blank shape

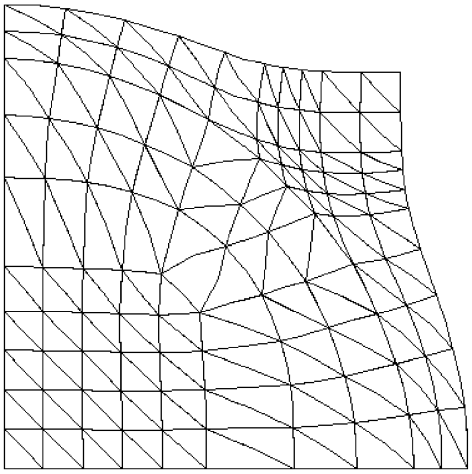

Fig. 15 Analysis result by FAST-3D program

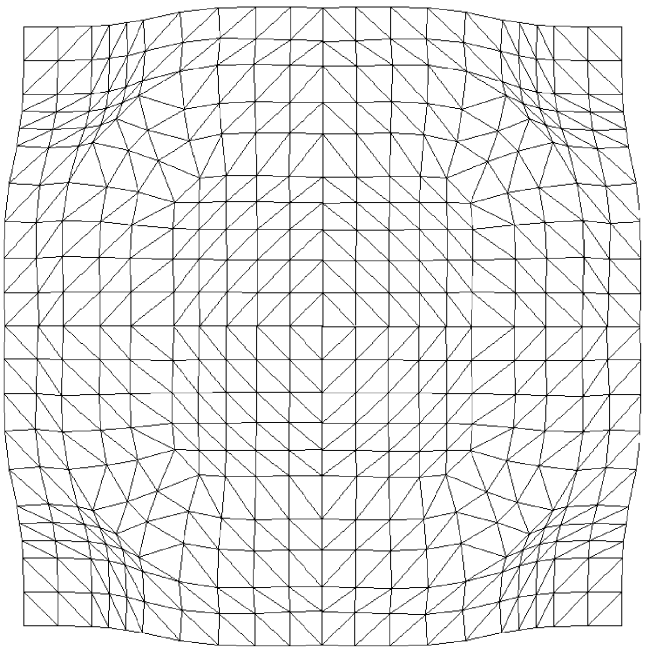

Fig. 16 Combined total initial blank shape

Figure 20 shows the initial blank shape of the front fender calculated by FAST-3D. As compared with Fig. 19, we can find that the result of the developed program is similar to the result obtained with FAST-3D, but the accuracy is not yet enough.

The reason for this difference seems to be that the area and volume of elements is not exactly calculated. Therefore, the program should be updated in future research.

4.3 Application to a Rear Hinge

In this section, the rear hinge is analyzed by using the one-step analysis. The rear hinge is one of the most important parts that make up the body of an automobile, and it has a very complex geometry, steep slope, sharp edge, and corners. Consequently, it is not easy to analyze the rear hinge, and the computation time also takes longer. Figure 21(a) shows the finite element mesh geometry of the rear hinge, and the material property is shown in Table 4. As a result of calculation, the initial blank shape is represented in Fig. 21(b), and Fig. 22 shows the initial blank shape of the rear hinge calculated by FAST-3D. A comparison between the initial blank predicted by the FAST-3D code and the initial blank calculated by the developed one-step program is shown in Fig. 23. Some difference occurred between the two contours. This appearance can be explained by the fact that an exact calculation of area and volume is not conducted.

Fig. 17 Tool surface for a fender

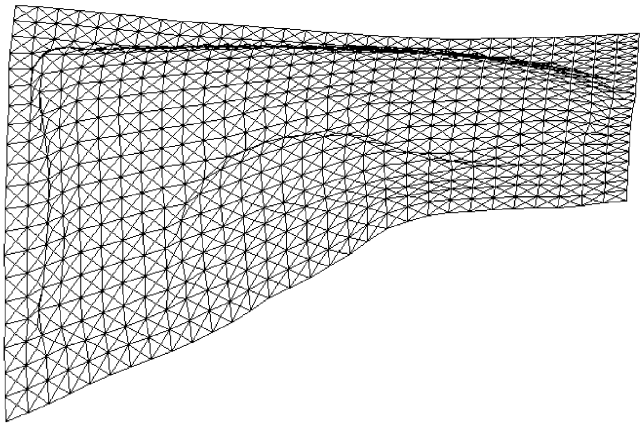

Fig. 18 Finite element mesh geometry of the front fender

Table 3 Material property (fender)

Initial material Thickness	*n* value	*r* value	Number of nodes	Number of element
1.2 mm	0.306	1.7	1251	2400

5. Conclusions

An explanation of the one-step FEM was described in this paper, and the developed program was applied to basic square

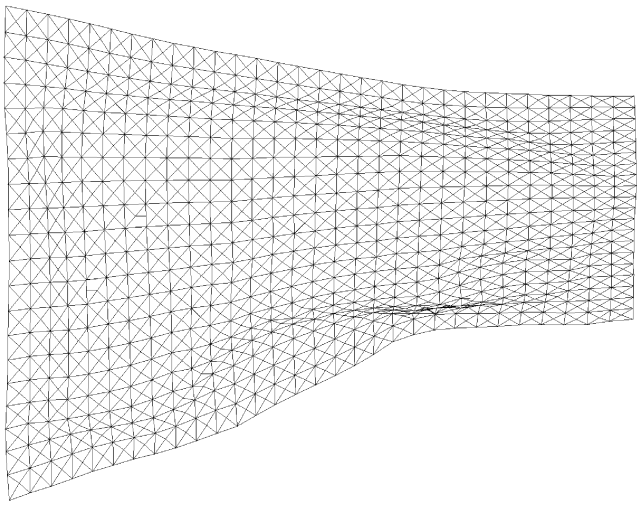

Fig. 19 Estimated initial blank shape by the developed program

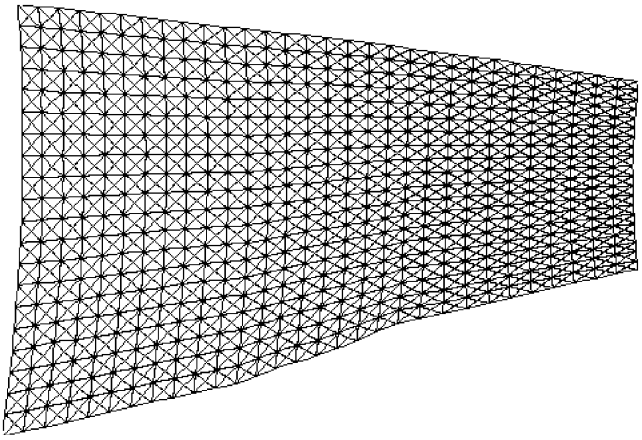

Fig. 20 Calculated initial blank shape by FAST-3D program

cup shape and actual automobile panels. Its availability was demonstrated through a comparison with the commercial program. The following conclusions could be induced from the results presented in this paper.

- If the one-step approach method is used in the sheet metal process, the computation time for the analysis will be reduced. In particular, this one-step approach is a very effective method for the product design process, which needs a short lead time.
- The initial blank shape of the sheet metal products was calculated by using the developed one-step program. We expect that the initial blank shape will provide practical help in the production process, because it can reduce a loss of material and working hours needed for trimming.
- The one-step approach method considers only two configurations, *i.e.*, initial blank shape and final shape. Therefore, the accuracy of the analysis method needs to be improved, and the analysis of frictional condition, bending, blankholding force, drawbead, *etc.* should be considered.

(a)

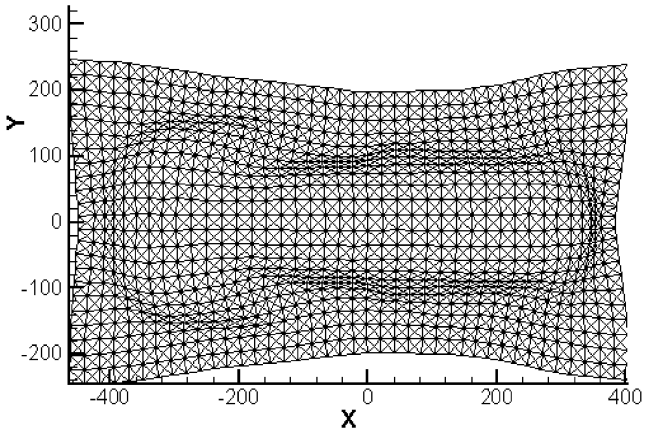

(b)

Fig. 21 Rear hinge model. **(a)** Final shape. **(b)** Calculated initial blank shape by the developed program

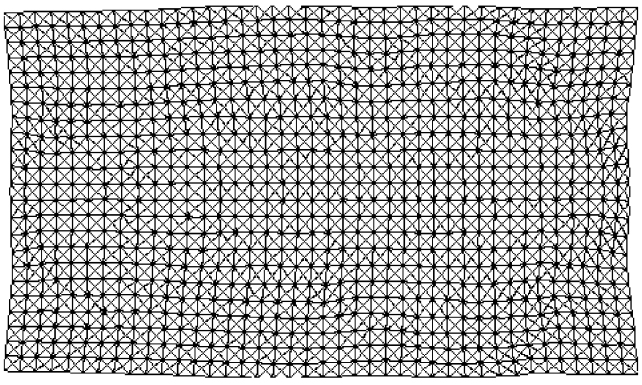

Fig. 22 Calculated initial blank shape by FAST-3D

Table 4 Material property (rear hinge)

Initial material Thickness	*n* value	*r* value	Number of nodes	Number of element
0.71 mm	0.185	1.45	1904	3680

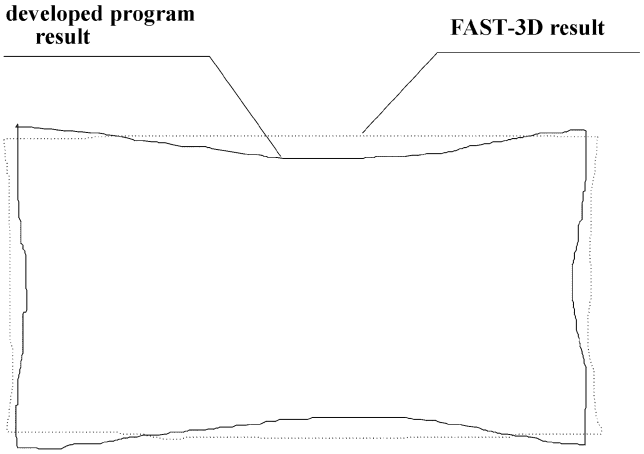

Fig. 23 Comparison of the FAST-3D and the developed program result

- The developed one-step program in this study has a tendency to allow the area and volume of element to be calculated inaccurately in the case of irregularly meshed shape and severe curvature problems. Therefore, more in-depth study is required in future research to improve the accuracy of calculation.

References

1. S.D. Liu and M. Karima: *Proc. NUMIFORM'92,* J.L. Chenot, R.D. Wood, and D.C. Zienkiewicz, A.A. Balkema, Rotterdam, Brookfield, 1992, pp. 497-502.
2. V.V. Hazek and K. Lange: *Proc. 7th NAMRC,* Ann Arbor, MI, 1979, pp. 65-71.
3. J.Y. Chu and A.P. Dou: *Proc. 3rd ICTP,* Kyoto, Japan, 1990, vol. 3, pp. 1319–24.
4. T. Kuwabara, W. Si, and M. Shuuno: *J. JSTP,* 1995, vol. 37 (422), pp. 290-96.
5. J.H. Vogel and D. Lee: *Int. J. Mech. Sci.,* 1990, vol. 32, pp. 891.
6. X. Chen and R. Sowerby: *Int. J. Mech. Sci.,* 1992, vol. 34 (2), pp. 159-66.
7. S.D. Kim, N.H. Park, and D.G. Seo: *Trans. KSTP,* 1995, pp. 302-21.
8. J.L. Batoz, Y.Q. Guo, P. Duroux, and J.M. Detraux: *NUMIFORM'89,* E.G. Thompson, R.D. Wood, D.C. Zienkiewicz, and A. Samuelsson, Fort Collins, A.A. Balkema, 1989, pp. 383-88.
9. S.H. Park: Master's Thesis, 373-1 Kusong-dong, Yusong-ku, Taejon, 305-701, Korea, 1996, pp. 18-20.
10. R. Sowerby, J.L. Duncan, and E. Chu: *Int. J. Mech. Sci.,* 1986, vol. 28(7), pp. 415-30.
11. K. Lange: *Hand Book of Metal Forming,* McGraw Hill, NY, 1985, pp. 20.48-20.49.
12. C.H. Lee: Ph.D. Thesis, 373-1 Kusong-dong, Yusong-ku, Taejon, 305-701, Korea, 1997, pp. 9-20.
13. R. Hill: *Math. Proc. Camb. Phil. Soc.,* 1979, vol. 85, pp. 179-91.
14. K. Chung and O. Richmond: *Int. J. Mech. Sci.,* 1992, vol. 34(7), pp. 575-91.